Biotechnol Lett (2024) 46:249–261
https://doi.org/10.1007/s10529-023-03459-8

ORIGINAL RESEARCH PAPER

# Silica nanoparticles enhance the cyto- and hemocompatibility of a multilayered extracellular matrix scaffold for vascular tissue regeneration

**Leslie A. Goldberg · Helena D. Zomer · Calum McFetridge · Peter S. McFetridge**

Received: 17 April 2023 / Revised: 4 November 2023 / Accepted: 14 December 2023 / Published online: 27 January 2024


## Abstract

*Purpose* The limited availability of autologous vessels for vascular bypass surgeries is a major roadblock to treating severe cardiovascular diseases. Based on this clinical priority, our group has developed a novel engineered vascular graft by rolling human amniotic membranes into multilayered extracellular matrixes (ECM). When treated with silica nanoparticles (SiNP), these rolled scaffolds showed a significant improvement in their structural and mechanical properties, matching those from gold standard autologous grafts. However, it remained to be determined how cells respond to SiNP-treated materials. As a first step toward understanding the biocompatibility of SiNP-dosed biomaterials, we aimed to assess how endothelial cells and blood components interact with SiNP-treated ECM scaffolds.

*Methods* To test this, we used established in vitro assays to study SiNP and SiNP-treated scaffolds' cyto and hemocompatibility.

*Results* Our results showed that SiNP effects on cells were concentration-dependent with no adverse effects observed up to 10 µg/ml of SiNP, with higher concentrations inducing cytotoxic and hemolytic responses. The SiNP also enhanced the scaffold's hydrophobicity state, a feature known to inhibit platelet and immune cell adhesion. Accordingly, SiNP-treated scaffolds were also shown to support endothelial cell growth while preventing platelet and leukocyte adhesion.

*Conclusion* Our findings suggest that the addition of SiNP to human amniotic membrane extracellular matrixes improves the cyto- and hemocompatibility of rolled scaffolds and highlights this strategy as a robust mechanism to stabilize layered collagen scaffolds for vascular tissue regeneration.

**Keywords** Cardiovascular disease · Coronary artery disease · Vascular graft · Amniotic membrane · Adhesive · Biocompatibility

Leslie A. Goldberg and Helena D. Zomer have contributed equally to this work.

**Supplementary Information** The online version contains supplementary material available at https://doi.org/10.1007/s10529-023-03459-8.

L. A. Goldberg · C. McFetridge · P. S. McFetridge (✉)
J. Crayton Pruitt Family Department of Biomedical Engineering, University of Florida, Biomedical Sciences Building JG-56, 1275 Center Drive, Gainesville, FL 32611-6131, USA
e-mail: pmcfetridge@bme.ufl.edu

H. D. Zomer
Department of Physiological Sciences, University of Florida, Gainesville, FL, USA

## Introduction

Coronary heart disease is the most common type of cardiovascular disease. In the United States, 600,000

new cases arise each year, with costs exceeding 5.5 billion dollars (Russell et al. 1998; Cheryl et al. 2012, 2020; Heron 2021; Virani et al. 2021). Although less invasive interventions are advancing, the highest survival advantage is achieved with heart bypass grafting, particularly in patients with ventricular dysfunction (Caines et al. 2004). Small diameter (< 6 mm) vascular reconstructions are considerably more challenging than larger vessels, due to low flow and high resistance that amplify poor host tissue/graft interactions. Autologous arteries are considered the gold standard for small-diameter replacement vessels, with patency rates of ~ 90% at five years (Pashneh-Tala et al. 2016; Mallis et al. 2020). Unfortunately, in approximately 30% of vascular reconstructions, the patient's own vessels are unavailable for use, requiring either a synthetic conduit or a non-operative approach to restore blood flow (Carrabba and Madeddu 2018). Issues with the peripheral vasculature have similar complications (Tukiainen et al. 2006; Ambler and Twine 2018).

More traditional synthetic alternatives such as modified Dacron or expanded polytetrafluoroethylene are limited to peripheral uses due to their low patency rates (Tiwari et al. 2002; Bota et al. 2010; Mrówczyński et al. 2014; Ambler and Twine 2018). These relatively inert materials remain problematic due to their inability to interact successfully with the recipient tissues, resulting in a complex set of adverse biological reactions, driven by poor biocompatibility and miss-matched mechanical properties (Schmidt and Bowlin 1999; Pashneh-Tala et al. 2016; Zhuang et al. 2021). Approaches to improve the current situation include the development of novel materials, including synthetic surfaces, biological grafts, and tissue-engineered vessels (L'heureux et al. 1998; Langer 2000; Dardik et al. 2002; Ozawa et al. 2002; Boura et al. 2003).

Our group developed a novel engineered vascular graft derived from the human amniotic extracellular matrix that can be customized to achieve matched wall thickness and any given internal diameter (Amensag and McFetridge 2012, 2014). When implanted in a rabbit model of vascular bypass, these rolled, tubular scaffolds showed adequate mechanical integrity, postoperative immunologic tolerance lasting at least four weeks, and evidence of cellular remodeling resembling the native vascular architecture (Amensag et al. 2017). However, the layers of these rolled scaffolds had a propensity to unravel upon hydration and during the surgical procedure where the graft required physical manipulation to suture in place. As such, these acellular grafts required overly delicate handling to prevent unraveling prior to closure. To solve this issue, we tested the potential for silica nanoparticles (SiNP) as a binding agent to adhere and reinforce the layers of these extracellular scaffolds (Goldberg et al. 2023—accompanying article in this Journal). Our Results showed that SiNP enhanced the self-adhesion between distinct layers and within individual layers of the rolled scaffolds, effectively improving the scaffold's tensile strength and handling properties (Goldberg et al. 2023). Our studies indicated that SiNP can be used as an effective adhesive for ex-vivo derived tissue scaffolds, with promising potential for tissue engineering and regenerative medicine applications requiring a biocompatible adhesive.

Although silica has been recognized as essentially nontoxic and safe by the FDA (Zhang et al. 2012; Gonçalves 2018), most medical applications of SiNP are still under study (Janjua et al. 2021). Therefore, the biocompatibility of SiNP-treated scaffolds where the SiNP are at the blood interface requires further assessment to ensure their clinical applicability as vascular grafts. The aim of this study was to assess how endothelial cells and blood components interact with the multilayered SiNP-treated scaffolds, as a first step toward the investigation of SiNP materials' broader biocompatibility.

## Materials and methods

### HUVECs isolation and culture

Placental tissues were obtained from the Labor & Delivery department at UF Health Shands Hospital at the University of Florida (Gainesville, FL, IRB Approval #64-2010). Human umbilical vein

endothelial cells (HUVECs) were isolated from umbilical cords using collagenase perfusion as described by Jaffe et al. (1973). Prior to reaching confluence, cells were passaged using Accutase with 0.5 mM EDTA (Innovative Cell Technologies). Experiments used mixed cell populations collected from at least three donor cords. Media was replaced every two to three days with VascuLife basal medium supplemented with VEGF (LifeLine Cell Technologies) and 100 U/ml penicillin/streptomycin. HUVECs were used experimentally between passages P2 and P4.

### Cytocompatibility of silica nanoparticles

Commercially available colloidal silica nanoparticles (Ludox TM-50, Sigma) were used in a range of dilutions as previously described (Goldberg et al. 2023). For the qualitative assessment of cell viability, we used a Live/Dead cell viability assay according to the manufacturer's protocol (Invitrogen). Briefly, 50,000 HUVECs (P4) were seeded into each well of 24-well plates. After cells reached a confluent monolayer, the culture medium was replaced with freshly prepared 0.5 ml nanoparticle dispersions diluted in the culture medium (0.1 µg/ml, 1 µg/ml, 10 µg/ml, 100 µg/ml, and 1000 µg/ml). Cells without exposure to nanoparticles (0 µg/ml) served as a control. Cells were incubated for 24 h at 37 °C in a 5% $CO_2$ incubator. Then, the media containing nanoparticles was aspirated from the wells and the cells were gently washed with PBS and stained with Calcein AM (green; living cells), ethidium homodimer-1 (red; dead cells), and DAPI (blue; cell nuclei). All conditions were performed in triplicate.

Cellular metabolic activity was assessed using the Alamar Blue assay (AB; Invitrogen, USA) per manufacturer's instructions. The percent reduction of resazurin to resorufin was used as an indicator of cellular metabolic activity. HUVECS plated as described above were washed with PBS and incubated with 10% Alamar Blue in media for four hours at 37°C to quantify relative metabolic activity. Supernatants were collected and fluorescence was read at excitation 530 nm, and emission 590 nm by a Synergy 2 multi-detection microplate reader (BioTek Instruments, Inc., Winooski, Vermont, USA). Percent reduction data were normalized to the control (0 µg/ml SiNP) and presented as percent cell viability.

### Blood collection and processing

Human venous blood was collected from healthy adult volunteers who had given their IRB-approved informed consent (IRB #642010). Blood (50 ml) was collected in tubes containing 10 U of heparin per ml using a 21-gauge needle and carefully handled before use to avoid activation of platelets and lysis of red blood cells. All participants acknowledged they had not taken medication that alters platelet function in the ten days before blood collection.

### Hemolysis test

The hemolysis test was performed as described previously (Zhao et al. 2011). Whole blood was centrifuged to separate the red blood cells from the buffy coat and plasma (800 g for 10 min). Red blood cells were diluted in the ratio of 1:20 in PBS to create a hematocrit of approximately 5%. Then, 200 µL of the red blood cell solution were incubated with 800 µL of freshly prepared SiNP dispersions diluted in PBS (0.1 µg/ml, 1 µg/ml, 10 µg/ml, 100 µg/ml, and 1000 µg/ml). Samples prepared with 800 µL of water and PBS served as positive and negative controls, respectively. Samples were incubated at room temperature under gentle agitation for two hours and subsequently centrifuged at 200×*g* for 5 min. Ruptured RBCs stained the supernatant red by the release of hemoglobin. The absorbance of the supernatant at 541 nm was used to quantify the percent of lysed RBCs using the following formula:

$$\%\ \text{hemolysis} = 100 \times \frac{(\text{absorbance of the sample} - \text{negative control sample})}{(\text{positive control absorbance} - \text{negative control absorbance})}$$

Preparation of silica nanoparticle treated-scaffolds

Layered rolled scaffolds derived from human amniotic membranes were prepared with SiNP in a range of concentrations or pH-matched phosphate buffer saline (PBS) as previously described (Amensag and McFetridge 2014; Meddahi-Pellé et al. 2014). Briefly, amniotic membranes were obtained from the Labor and Delivery Department at UF Health Shands Hospital at the University of Florida (Gainesville, FL, IRB Approval #64-2010), decellularized, and cut into 6 cm × 10 cm rectangular sheets for rolling. Flat, rectangular sections of the amnion were coated with either SiNP dispersions or pH-matched phosphate buffer saline (PBS). Amnion sections were laid flat on a sterile surface with any folds removed to maintain uniformly flat surface. The total volume of SiNP (or controls) was calculated based on the surface area of the scaffold whereby a uniform film would cover the entire surface (5 µl/cm$^2$). The sheet was then tightly rolled for ten revolutions around a 3.2 mm diameter mandrel. Rolled scaffolds were frozen at -86 °C for 12 h, then lyophilized within a Millrock Bench-Top Freeze-Drier (Millrock Technology, Kingston, NJ) and freeze-dried between 4 and 8 mT for 24 h.

Water contact angle

Scaffolds' wettability, or hydrophobicity, was determined by the sessile droplet method (Arasteh et al. 2016) The contact angle of distilled water droplets placed on scaffolds prepared with 0 µg/mm$^2$, 8.75 µg/mm$^2$, 17.5 µg/mm$^2$, 35 µg/mm$^2$, and 70 µg/mm$^2$ SiNP was determined as follows. Briefly, 10-layered scaffolds were opened along the longitudinal axis using a scalpel and fixed to a base with the luminal surface facing up. Drops of distilled $H_2O$ (25 µL) were pipetted onto the luminal surface of the scaffold and immediately photographed using a Nikon D200 (Melville, NY). The angle at the interface of the droplet and scaffold surface was quantified using NIH ImageJ software (Bethesda, MD).

Cytocompatibility of SiNP scaffolds

Ten-layered scaffolds treated with 8.75 µg/mm$^2$ SiNP were opened longitudinally and then cut into 1 cm × 1 cm sections. The dose used was defined based on optimal responses obtained in our mechanical characterization studies as described in the accompanying article in this Journal (Goldberg et al. 2023). Scaffolds were placed in 24-well plates, hydrated in PBS, and seeded on the luminal side with HUVECs (50,000 cells/well). After allowing cells to adhere overnight, seeded constructs were transferred into fresh wells (such that the cells adhered to the well plate would not interfere with the results of the subsequent study). Cells were cultured for 14 days, with media replaced every two to three days. The metabolic activity was assayed using Alamar Blue as described above on days 1, 2, 5, 7, and 14. Results are shown as the percent change in metabolic activity normalized to day 1 activity.

Dynamic evaluation of platelet-material interaction

For the dynamic evaluation of platelet-material interactions, whole blood was fluorescently labeled using acridine orange (20 µg/ml, 10 min incubation, Invitrogen). A syringe pump perfused a steady, laminar flow of blood over the scaffolds for 5 min in a custom-designed tissue-based parallel plate flow chamber that accommodates tissue surfaces and real-time visualization in a fluorescent microscope through a transparent viewing window to study scaffold-cell interactions (Uzarski et al. 2014). The flow rate was 1 ml/min to achieve shear stress of 10 dyn/cm$^2$. Samples were visualized on Zeiss AxioImager M2 upright fluorescence microscope with a Zeiss AxioCam Hrm Rev 3 digital camera operated by AxioVision software version 4.8. Images were taken from 15 locations along the length of the scaffold at 15-s intervals, for a total of five minutes. NIH ImageJ software was used to quantify the number of platelet aggregations (defined as a grouping of three or more platelets, and assumed to be caused by activated platelets), and percent coverage (by utilizing thresholding in NIH ImageJ software).

Leukocyte attachment assay

HL-60 cells (a human promyelocytic leukemia cell line) transfected with a lentiviral vector expressing green fluorescent protein (GFP), generously donated by Dr. Christopher Cogle at the University of Florida, were induced to differentiate towards neutrophil-like phenotypes by adding 1.3% dimethyl sulfoxide (DMSO) to the culture medium for three days.

Scaffolds were cut longitudinally (8 cm × 1 cm) and mounted into a custom-modified parallel plate flow chamber with the luminal surface facing up. Differentiated HL-60 cells (20,000 cells/cm$^2$) were incubated on the scaffolds for five hours at 37 °C and then imaged at 15 locations along the scaffold. Then, the chambers were perfused with PBS for five minutes at a constant rate of 1 ml/min to achieve a shear stress of 10 dyn/cm$^2$. After five minutes, the scaffold was again imaged at 15 locations. Neutrophil attachment was quantified from the images using ImageJ software (NIH).

### Statistical analysis

Experiments were run in no less than three replicates. Results are reported as mean ± standard deviation. One-way ANOVA was used to determine differences between scaffolds treated with different concentrations of nanoparticles. When ANOVA detected significance, Tukey post-hoc analysis was used to determine significant differences between each tested condition. Student t-test was used when only one condition was evaluated against a control. Statistical significance was set at $P < 0.05$.

## Results

### Cytotoxicity and hemolysis induced by silica nanoparticles are concentration-dependent

In order to gain insight into the cytocompatibility of SiNP, we first exposed HUVECs cultured in 24-well culture plates to a range of SiNP concentrations (Fig. 1). Cell viability and metabolic activity were unaffected at concentrations up to 10 µg/ml. However, at higher concentrations, cytotoxicity was observed ($P < 0.05$). At 100 µg/ml, approximately 50% of the cells were viable, and at 1000 µg/ml, no viable cells were detected.

To evaluate hemocompatibility, we incubated red blood cells with nanoparticle solutions to test if SiNP induced hemolysis. Disruption of erythrocyte membranes results in hemoglobin release into solution, so that nanoparticle-induced blood cell damage can be evaluated by quantifying free hemoglobin. No detectable red blood cell lysis was seen in samples with concentrations up to 10 µg/ml (Fig. 2). Hemolysis was observable starting at 100 µg/ml (1.7% hemolysis, not significantly different than controls) and markedly increased at 1000 µg/ml (63% hemolysis, $P < 0.05$). Taken together, these findings suggest that SiNPs are nontoxic to erythrocytes in concentrations up to 10 µg/ml.

### Silica nanoparticle-enhanced scaffolds are hydrophobic

Using in vitro analysis we aimed to evaluate the applicability of the SiNP treated 10-layered scaffolds as vascular grafts by assessing the surface hydrophobicity, known to influence platelet/biomaterial adhesion (Jaffer and Weitz 2019; Wu et al. 2021). The contact angle of water droplets placed on scaffolds was assessed over a range of SiNP concentrations from 0 µg/mm$^2$ (control), 8.75 µg/mm$^2$, 17.5 µg/mm$^2$, 35 µg/mm$^2$, to 70 µg/mm$^2$ (Fig. 3). Results show untreated scaffolds were hydrophilic (contact angle < 90°), with a mean contact angle of 74° ± 10°, whereas all scaffolds treated with SiNP were progressively more hydrophobic as the concentration of SiNP increased ($P < 0.001$). These findings indicate that the addition of SiNP to extracellular matrix scaffolds improves their hemocompatibility properties by decreasing the surface free energy.

To verify the cytocompatibility of the ten-layered SiNP-treated scaffolds, samples were prepared with 8.75 µg/mm$^2$ either with or without (controls) SiNP, then cut into 1 cm$^2$ sections (Fig. 4a) and cultured with HUVECs for 14 days. From day 5 of culture and onwards, HUVECs showed increased metabolic activity on SiNP-treated scaffolds in comparison to day 1, and when compared to cells seeded in untreated scaffolds (Fig. 4b). This result demonstrates that the presence of SiNP in extracellular-matrix scaffolds may improve the environment for cell growth.

### Silica nanoparticles inhibit platelet and leukocyte adhesion

The evaluation of platelet aggregation over time revealed that SiNP-treated scaffolds inhibit platelet aggregation in comparison to untreated scaffolds ($P < 0.05$) for at least 3 min (Fig. 5a, b). In this period, treated scaffolds also showed smaller and

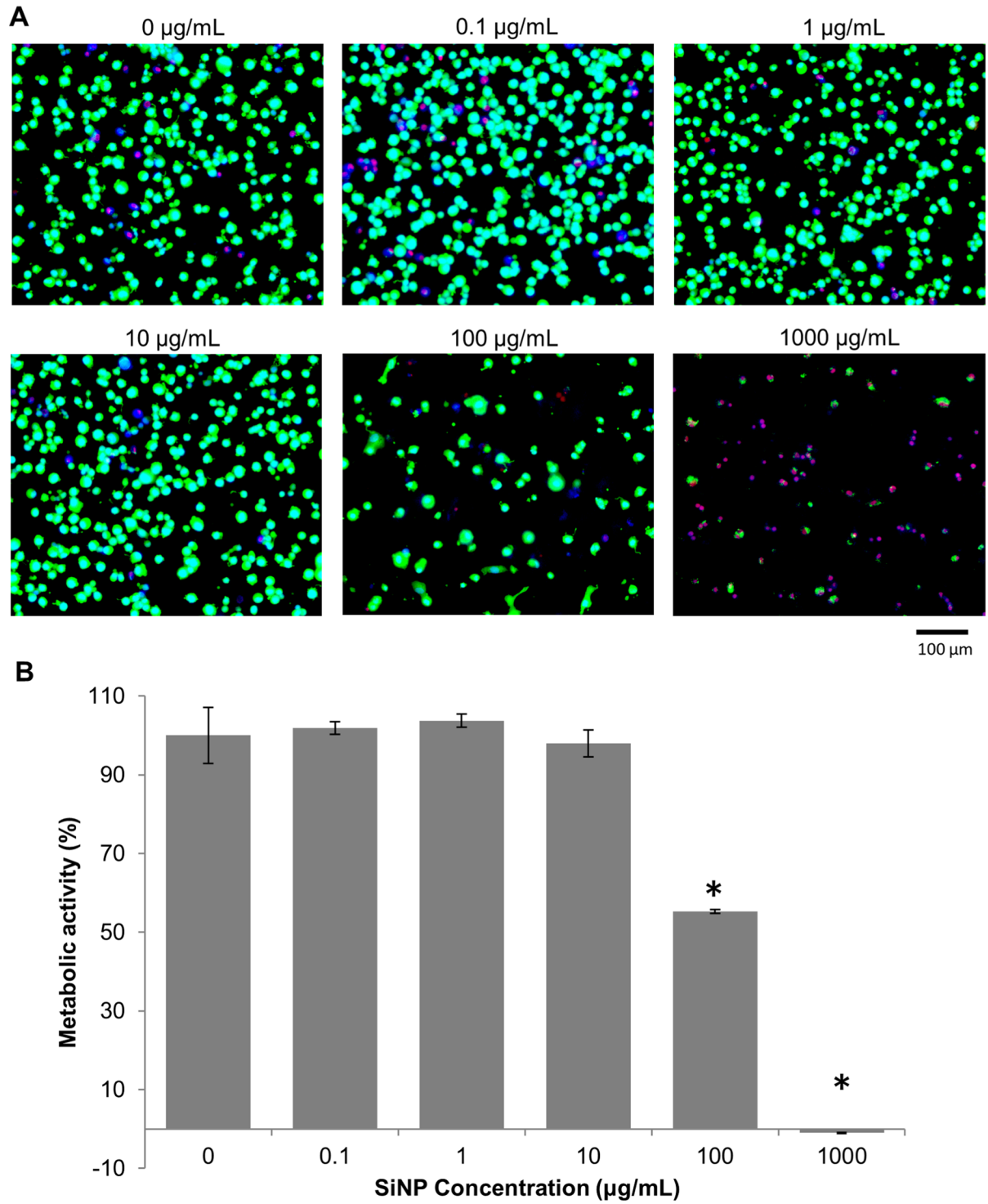


**Fig. 1** Cytotoxicity of silica nanoparticles. HUVECs were exposed to a range of SiNP concentrations for 24 h. **a** Cell viability was assessed by Live/Dead stain. Images show viable cells (green), dead cells (red), and cell nuclei (blue). **b** Cellular metabolic activity in relation to untreated controls. Cytotoxicity was observed at 100 and 1000 µg/ml. *$P < 0.05$ by one-way ANOVA

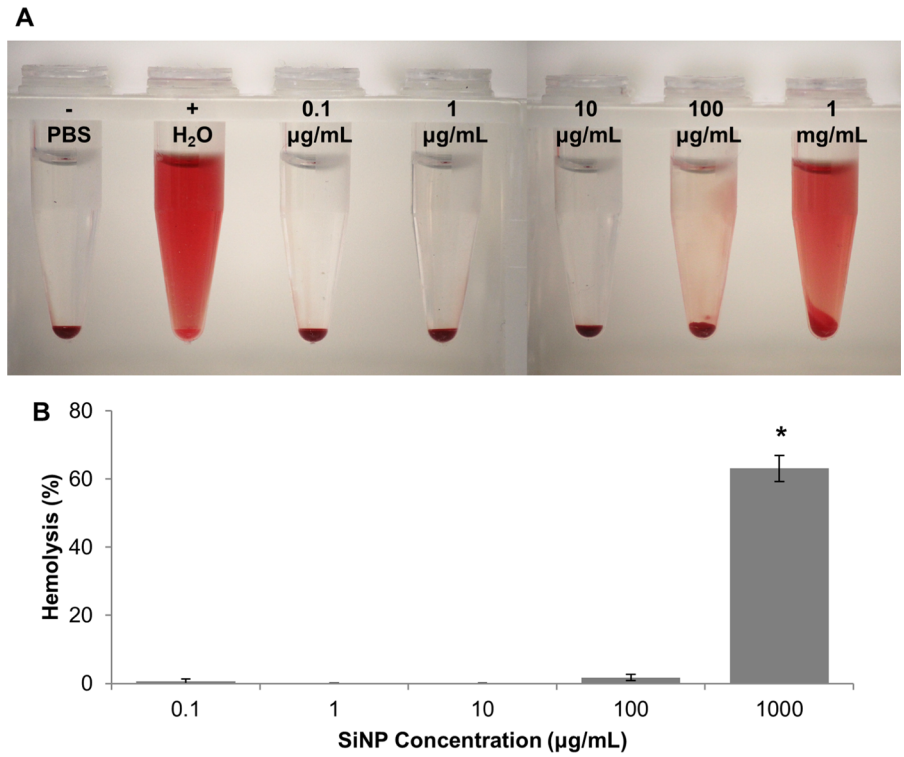


**Fig. 2** Hemolysis induced by silica nanoparticles. **a** Representative photographs of hemolysis over a range of SiNP concentrations. The hemoglobin is released into the supernatant when red blood cell membrane integrity is compromised. Negative (PBS) and positive (water) controls are shown on the left. **b** Percent of hemolysis was determined by the absorbance of the supernatant at 541 nm. *P < 0.05 by one-way ANOVA

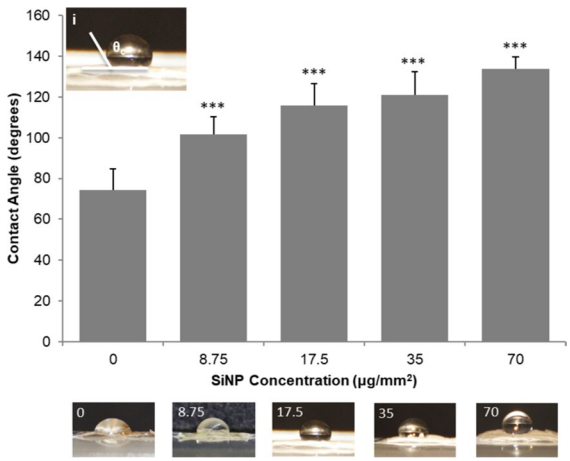


**Fig. 3** Hydrophobicity of SiNP-enhanced scaffolds. A water droplet was placed on top of scaffolds prepared with increasing nanoparticle concentrations. The surface contact angle was measured as shown in insert (i). Average contact angle and representative photographs of water droplets of each condition are shown. ***P < 0.001 by one-way ANOVA Silica nanoparticles-enhanced scaffolds support cell growth

fewer aggregates than controls (Fig. 5c), indicating an initial lower activation state. However, both treated and untreated scaffolds reached similar values for percentage coverage and aggregate size after 4 and 5 min. Nevertheless, the total percentage of platelet coverage in all scaffolds was below 3.5% by the end of the 5 min.

To further evaluate SiNP hemocompatibility, HL-60 cells differentiated into neutrophils were seeded on scaffolds for five hours and perfused with saline for five minutes at 10 dyn/cm$^2$ to test leukocyte adhesion (Fig. 6). Initial leukocyte attachment to the SiNP-treated and control scaffolds (5 h after seeding) were not statistically different. However, after 5 min of perfusion with a shear stress of 10 dyn/cm$^2$, 33% of cells detached from the SiNP-treated scaffolds, significantly more than in control scaffolds, where cells attached remained similar to values pre-perfusion. These findings suggest that leukocytes adhere weakly to SiNP-treated scaffolds.

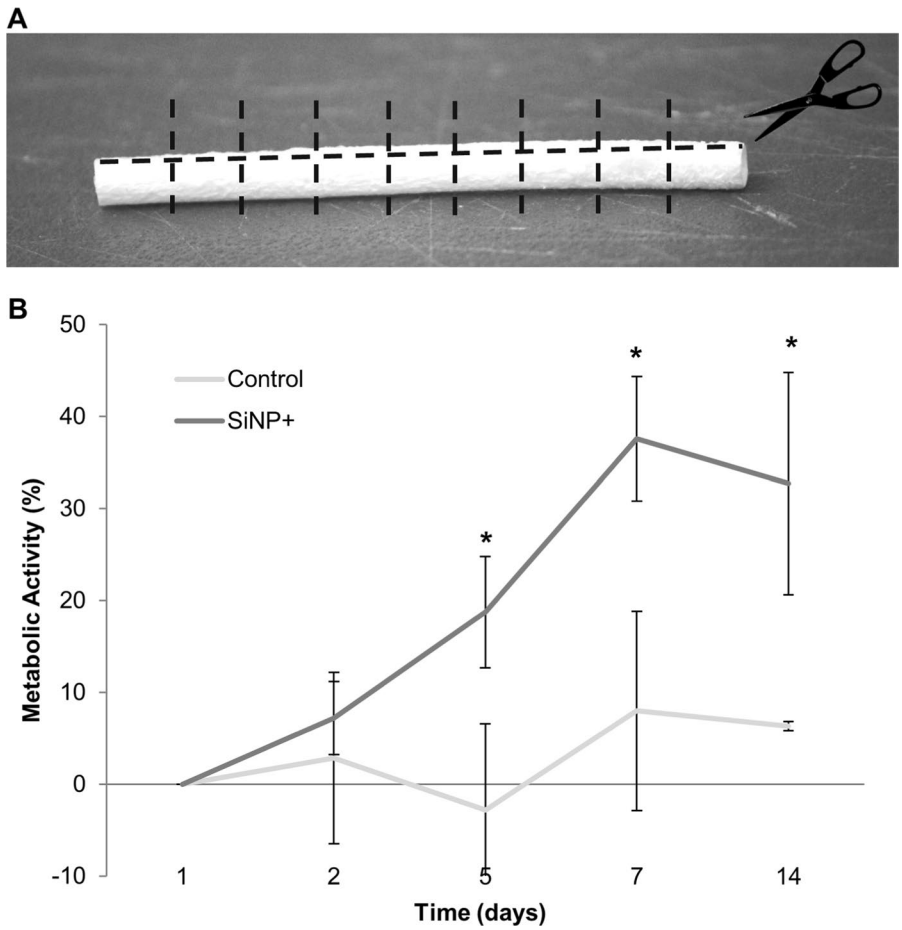


**Fig. 4** Cytotoxicity of SiNP-enhanced scaffolds. **a** 10-layered rolled scaffolds treated with 8.75 µg/mm$^2$ SiNP and untreated controls were sectioned as shown and cultured with HUVEC for 14 days. **b** Cellular metabolic activity was tested at different time points. The percentage of metabolic activity was determined in relation to day 1 of culture. Cells cultured on SiNP-enhanced scaffolds presented overall higher metabolic activity than untreated controls. *P < 0.05 by T-test (Control × SiNP in each time point)

## Discussion

With a significant clinical need for vascular bypass grafting materials with improved patency rates, a novel vascular graft comprised of prepared human amniotic membrane treated with SiNP to create a robust multiple layered vascular graft has been developed. An advantage of this approach over currently clinically available grafts is that the scaffold can be readily modified to alter the materials diameter, thickness, and length to suit a variety of vascular reconstruction needs. As a critical component of this development, the compatibility of the composite biomaterial (ECM-SiNP), is required. While silica is recognized as essentially nontoxic and safe by the FDA, and has its use approved for multiple applications in the food industry, dentistry, orthopedics, ophthalmology, and dermatology (Zhang et al. 2012; Gonçalves 2018), the biocompatibility of silica nanoparticles at the blood/surface interface of vascular grafts remains unknown. Herein, we aimed to assess endothelial and blood cell components' responses to the composite material.

In this study, the potential toxicity of SiNP on endothelial cells was evaluated with two approaches: (1) direct exposure of cultured HUVECs to an array of SiNP concentrations dispersed in the culture media, and (2) indirect exposure of cultured HUVEC on SiNP-treated rolled extracellular matrix scaffolds. Direct exposure showed that SiNP are not cytotoxic in concentrations up to 10 µg/ml. Furthermore, culturing HUVEC on scaffolds prepared with 8.75 µg/mm$^2$ SiNP demonstrated no apparent toxicity to the cells, and cell growth was supported for at least 14 days. As the rolled amniotic extracellular matrix is composed of tightly packed fibers with subcellular sized pores, seeded HUVEC remain on the luminal surface of the material while SiNP are largely retained

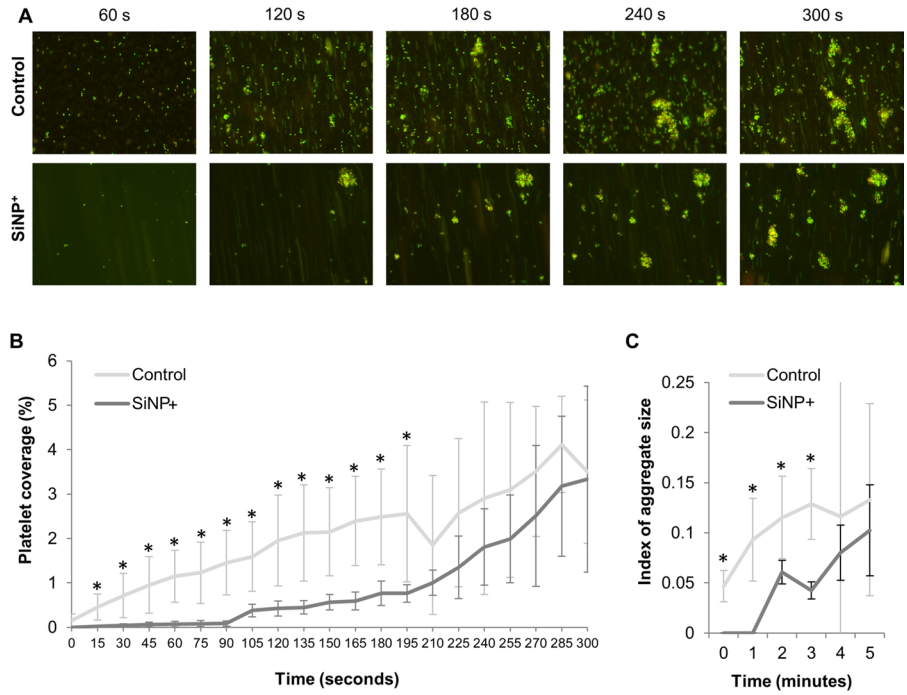


**Fig. 5** Dynamic Evaluation of Platelet-Material Interaction. Whole blood was stained with acridine orange and flowed through the scaffold at 10 dyn/cm$^2$. Platelet attachment and aggregation were evaluated for 5 min. **A** Representative photographs of blood cells adhered to control and SiNP-treated scaffolds (8.75 µg/mm$^2$). **B** Dynamic quantification of platelet surface coverage. **C** Index of aggregate size was determined by the percentage of surface coverage normalized by the number of aggregations. *P < 0.05 by T-test (Control × SiNP in each time point)

between each layer of the rolled scaffold (Supplemental Fig. 1). This organization presumably protects the cells by avoiding excessive direct contact with SiNP.

The use of natural extracellular matrixes as a platform for tissue engineering is advantageous as they are biodegradable without toxic breakdown products. However, when SiNP-treated scaffolds are degraded, SiNP may ultimately be released into the bloodstream. Herein we show that SiNP do not cause hemolysis when in direct contact with blood in concentrations up to 10 µg/ml, with minimum hemolysis induced even at 100 µg/ml. As progressive scaffold remodeling occurs in the host, SiNP release is expected to be gradual rather than abrupt, so these tested doses are likely significantly higher than those that would be experienced in vivo. Although the in vitro system has limited translation to the complex, in vivo environment, these findings suggests that SiNP-treated scaffolds are not overtly toxic for red blood cells or other peripheral blood cells.

Small-diameter bypass vessels are especially prone to failure by occlusive thrombus formation (Wang et al. 2007). Whereas the native vasculature has inherent anti-thrombotic mechanisms such as a confluent endothelial cell layer, damages to the endothelium, including those surgically induced, trigger a coagulation cascade that leads to exposure of the subendothelial extracellular matrix and consequent platelet binding and activation (Chen and López 2005). Activated platelets release factors that bind and activate more platelets resulting in aggregation and potential clot formation (Menter et al. 2017). This naturally occurring hemostatic response to vascular injury is kept in balance by factors secreted from quiescent endothelial cells (Chen and López 2005; Coller and Shattil 2008). In this sense, an adequate vascular graft surface must induce minimal platelet adhesion and activation in order to minimize thrombotic events (Jaffer et al. 2015).

It has been shown that surface hydrophobicity plays an important role in the hemocompatibility of materials as it influences protein adsorption and thus thrombogenicity (Shabalovskaya et al. 2013). Herein, we found that the addition of SiNP modifies the scaffold's surface properties from hydrophilic to hydrophobic in a concentration-dependent manner. To detail these interactions we used a modified parallel plate flow chamber (Uzarski et al. 2014) to evaluate the dynamics of platelet-material interaction. As shear stress is known to influence both platelet adhesion and the coagulative response, (Furukawa et al. 2010) our approach using a unique

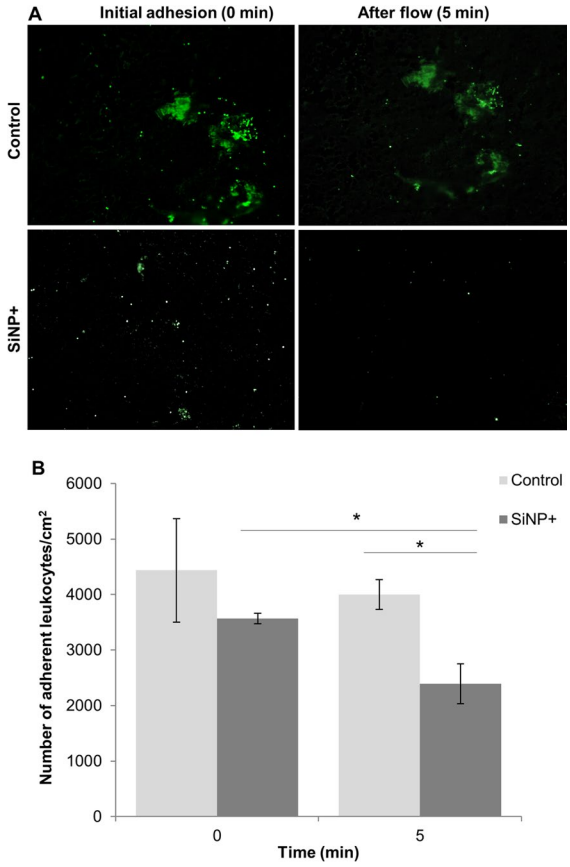


**Fig. 6** Leukocyte attachment. Leukocytes were cultured on untreated scaffolds (controls) or SiNP-treated scaffolds (8.75 µg/mm$^2$) for 5 h and then exposed to a constant saline flow (10 dyn/cm$^2$ for 5 min). Adhered leukocytes were quantified at time zero (initiation of flow) and at the final time point (5 min). **A** Representative photomicrographs of GFP + leukocytes (green) adhered to scaffolds. **B** Quantification of leukocytes attached to the scaffold surface. *P < 0.05 by T-test

flow chamber allows for the assessment of cell-material interactions in real-time under shear conditions, in contrast to previous studies that used static methods for measuring clotting time (Casa et al. 2015). By perfusing whole blood over the scaffolds, we found a significant decrease in platelet adhesion and aggregation (a marker of platelet activation) in SiNP-treated scaffolds. Plasma proteins, such as albumin and fibrinogen, mediate platelet adsorption to surfaces and participate in thrombus formation (Tsai et al. 2002). Considering that albumin and fibrinogen have small negative charges at physiological pH, they are expected to induce minimal adsorption to silica surfaces (Fukuzaki et al. 1996). This may explain, in part, how SiNP inhibit platelet aggregation. Of note, both SiNP-treated and non-treated control scaffolds showed similar platelet aggregation (less than 3.5% of coverage) after 5 min, and comparable to our previous findings in decellularized human umbilical vein scaffolds (Uzarski et al. 2014). Our results also support those previously reported by Amensag et al. with amnion graft patency seen in a rabbit model (Amensag et al. 2017) as well as by Kakavand et al. where amniotic membrane surfaces displayed minimal platelet activation and no hemolysis (Kakavand et al. 2017).

To further investigate SiNP hemocompatibility, we perfused a neutrophil solution over the scaffolds to evaluate neutrophil-mediated immune responses. We found that, at least in the short-term, the presence of SiNP reduced the adherence of neutrophils to the scaffolds. As neutrophils have been shown to play an important role in graft rejection (Cardozo et al. 2004), this finding indicates a beneficial effect of SiNP on the scaffold immunoregulatory properties.

In summary, we aimed to assess the responses of endothelial cells and peripheral blood cells to SiNP-treated extracellular matrix scaffolds. We showed that SiNP are well tolerated by endothelial cells and red blood cells in concentrations up to 10 µg/ml and the addition of SiNP increases the scaffolds' hydrophobicity, and decreases platelet aggregation and leukocyte attachment. Although we have identified a dose-dependent cytotoxicity and hemotoxicity of unaltered Ludox TM50 silica nanoparticles, toxic effects were only seen at substantially higher concentrations than those optimally defined to glue ECM scaffolds.

Similar in concept to the earlier work by L'Heureux et al. using 'cell sheet' technology to create layered structures, the technology described herein has used thin sheets of ECM derived from the human amniotic membrane(L'heureux et al. 1998; Amensag and McFetridge 2014).This approach has the advantages of being readily available, derived from human tissues and provide a 'natural structure' that includes a basement membrane with the potential to speed remodeling and aid endothelial cell function. It can be assembled to almost any vessel size and wall thickness by rolling the ECM sheets around a mandrel and rolling until the desired thickness is achieved. Importantly, and unlike most other biomaterials, it does not elicit an adverse immune reaction

whilst being fully remodelable by the body, this plus evidence of more than a century of clinical use make this membrane an ideal choice in the right applications (Hopkinson et al. 2006; Mamede et al. 2012; Walgenbach et al. 2012; Allen et al. 2013). While longer term stability studies in vivo are still required, this work demonstrates the approach to create a versatile off-the-shelf graft, with promising in vitro and in vivo performance (Amensag et al 2017).

In conclusion, these investigations have shown that SiNP are suitable for use as a 'glue' to bind layers of the amniotic extracellular matrix when rolled into 3D tubes for potential clinical use. The addition of SiNP in these concentrations is not only safe to endothelial and red blood cells, but also substantially improves their broader hemocompatibility properties. This study adds to our knowledge by providing a preliminary understanding of the biocompatibility of SiNP and SiNP-treated ECM-based grafts in the blood interface and supports its exploration in diverse vascular engineering applications. Nevertheless, this work is limited to in vitro analyses, so future animal studies are necessary to ensure biocompatibility in complex in vivo systems. The next steps of this work will use pre-clinical approaches to confirm these findings in animal models.

## Supplementary Information

**Supplemental Figure 1** Ultrastructure of SiNP-treated amniotic membrane rolled scaffolds. Scanning electron microscopy (a,b) and transmission electron microscopy (c,d) of scaffolds treated with 8.75 µg/mm2 SiNP. SiNP remained trapped between the layers of extracellular matrix (ECM).

**Acknowledgements** Special thanks to Kimberly Backer-Kelley of the Interdisciplinary Center for Biotechnology Research for her support at the Electron Microscopy core lab. UF Health Shands Labor & Delivery unit. Dr. Dara Wakefield and Louis Kauo of the UF Health Shands Department of Pathology.

**Author contributions** LAG: Performed experiments, analyzed the data and wrote the paper; HDZ: analyzed the data and wrote the paper; CMF: performed experiments, wrote the paper; PMF: Supervised the study, analyzed the data and wrote the paper.

**Funding** Financial support provided by the National Institute of Health (NIH R01 HL088207).

**Data availability** The data that support the findings of this study are available from the corresponding author upon reasonable request.

**Declarations**

**Conflict of interest** The authors have no conflict of interest to disclose.

**Ethical approval** Placental tissues were obtained from the Labor & Delivery department at UF Health Shands Hospital at the University of Florida (Gainesville, FL, IRB Approval #64-2010).

## References

Allen CL, Clare G, Stewart EA et al (2013) Augmented dried versus cryopreserved amniotic membrane as an ocular surface dressing. PLoS ONE. https://doi.org/10.1371/JOURNAL.PONE.0078441

Ambler GK, Twine CP (2018) Graft type for femoro-popliteal bypass surgery. Cochrane Database Syst Rev. https://doi.org/10.1002/14651858.CD001487.pub3

Amensag S, McFetridge PS (2012) Rolling the human amnion to engineer laminated vascular tissues. Tissue Eng Part C 18:903–912. https://doi.org/10.1089/ten.tec.2012.0119

Amensag S, McFetridge PS (2014) Tuning scaffold mechanics by laminating native extracellular matrix membranes and effects on early cellular remodeling. J Biomed Mater Res Part A 102:1325–1333. https://doi.org/10.1002/jbm.a.34791

Amensag S, Goldberg LA, O'Malley KA et al (2017) Pilot assessment of a human extracellular matrix-based vascular graft in a rabbit model. J Vasc Surg 65:839. https://doi.org/10.1016/j.jvs.2016.02.046

Arasteh S, Kazemnejad S, Khanjani S et al (2016) Fabrication and characterization of nano-fibrous bilayer composite for skin regeneration application. Methods 99:3–12. https://doi.org/10.1016/j.ymeth.2015.08.017

Bota PCS, Collie AMB, Puolakkainen P et al (2010) Biomaterial topography alters healing in vivo and monocyte/macrophage activation in vitro. J Biomed Mater Res Part A 95:649–657. https://doi.org/10.1002/jbm.a.32893

Boura C, Menu P, Payan E et al (2003) Endothelial cells grown on thin polyelectrolyte mutlilayered films: an evaluation of a new versatile surface modification. Biomaterials 24:3521–3530. https://doi.org/10.1016/S0142-9612(03)00214-X

Caines AEB, Massad MG, Kpodonu J et al (2004) Outcomes of coronary artery bypass grafting versus percutaneous coronary intervention and medical therapy for multivessel disease with and without left ventricular dysfunction. Cardiology 101:21–28. https://doi.org/10.1159/000075982

Cardozo LAM, Rouw DB, Ambrose LR et al (2004) The neutrophil: the unnoticed threat in xenotransplantation? Transplantation 78:1721–1728. https://doi.org/10.1097/01.TP.0000147341.40485.B4

Carrabba M, Madeddu P (2018) Current strategies for the manufacture of small size tissue engineering vascular grafts. Front Bioeng Biotechnol 6:41

Casa LDC, Deaton DH, Ku DN (2015) Role of high shear rate in thrombosis. Mosby, Maryland Heights

Center for Disease Control and Prevention, Underlying Cause of Death 1999-2020. (2020) [cited 11/01/2023]; Available from: https://wonder.cdc.gov/wonder/help/ucd.html

Chen J, López JA (2005) Interactions of platelets with subendothelium and endothelium. Microcirculation 12(3):235–246

Cheryl F, Chen T-C, Li X (2012) Prevalence of uncontrolled risk factors for cardiovascular disease: United States, 1999–2010. NCHS Data Br 103

Coller BS, Shattil SJ (2008) The GPIIb/IIIa (integrin άIIbB3) odyssey: a technology-driven saga of a receptor with twists, turns, and even a bend. Am Soc Hematol 112:3011–3025

Dardik H, Wengerter K, Qin F et al (2002) Comparative decades of experience with glutaraldehyde-tanned human umbilical cord vein graft for lower limb revascularization: an analysis of 1275 cases. J Vasc Surg 35:64–71. https://doi.org/10.1067/mva.2002.121053

Fukuzaki S, Urano H, Nagata K (1996) Adsorption of bovine serum albumin onto metal oxide surfaces. J Ferment Bioeng 81:163–167. https://doi.org/10.1016/0922-338X(96)87596-9

Furukawa KS, Nakamura K, Onimura Y et al (2010) Quantitative analysis of human platelet adhesions under a small-scale flow device. Artif Organs 34:295–300. https://doi.org/10.1111/j.1525-1594.2009.00862.x

Gonçalves MC (2018) Sol-gel silica nanoparticles in medicine: a natural choice. Design, synthesis and products. Molecules. https://doi.org/10.3390/molecules23082021

Heron M (2021) Deaths: leading causes for 2019. Natl Vital Stat Rep 70:1–114

Hopkinson A, McIntosh RS, Tighe PJ et al (2006) Amniotic membrane for ocular surface reconstruction: donor variations and the effect of handling on TGF-beta content. Invest Ophthalmol vis Sci 47:4316–4322. https://doi.org/10.1167/IOVS.05-1415

Jaffer IH, Weitz JI (2019) The blood compatibility challenge. Part 1: blood-contacting medical devices: the scope of the problem. Acta Biomater 94:2–10

Jaffe EA, Nachman RL, Becker CG, Minick CR (1973) Culture of human endothelial cells derived from umbilical veins. Identification by morphologic and immunologic criteria. J Clin Invest 52:2745–2756. https://doi.org/10.1172/JCI107470

Jaffer IH, Fredenburgh JC, Hirsh J, Weitz JI (2015) Medical device-induced thrombosis: what causes it and how can we prevent it? Wiley, New York

Janjua TI, Cao Y, Yu C, Popat A (2021) Clinical translation of silica nanoparticles. Nat Rev Mater 6:1072–1074. https://doi.org/10.1038/s41578-021-00385-x

Kakavand M, Yazdanpanah G, Ahmadiani A, Niknejad H (2017) Blood compatibility of human amniotic membrane compared with heparin-coated ePTFE for vascular tissue engineering. J Tissue Eng Regen Med 11:1701–1709. https://doi.org/10.1002/term.2064

Langer R (2000) Biomaterials: status, challenges, and perspectives. AIChE J 46:1286–1289

L'heureux N, Pâquet S, Labbé R et al (1998) A completely biological tissue-engineered human blood vessel. FASEB J 12:47–56. https://doi.org/10.1096/fasebj.12.1.47

Mallis P, Kostakis A, Stavropoulos-Giokas C, Michalopoulos E (2020) Future perspectives in small-diameter vascular graft engineering. Bioengineering 7:1–40. https://doi.org/10.3390/bioengineering7040160

Mamede AC, Carvalho MJ, Abrantes AM et al (2012) Amniotic membrane: from structure and functions to clinical applications. Cell Tissue Res 349:447–458. https://doi.org/10.1007/s00441-012-1424-6

Meddahi-Pellé A, Legrand A, Marcellan A et al (2014) Organ repair, hemostasis, and in vivo bonding of medical devices by aqueous solutions of nanoparticles. Angew Chem 53:6369–6373. https://doi.org/10.1002/anie.201401043

Menter DG, Kopetz S, Hawk E, et al (2017) Platelet "first responders" in wound response, cancer, and metastasis. NIH Public Access

Mrówczyński W, Mugnai D, De Valence S et al (2014) Porcine carotid artery replacement with biodegradable electrospun poly-e-caprolactone vascular prosthesis. J Vasc Surg 59:210–219. https://doi.org/10.1016/j.jvs.2013.03.004

Ozawa T, Mickle DAG, Weisel RD et al (2002) Optimal biomaterial for creation of autologous cardiac grafts. Circulation 106:I176–I182. https://doi.org/10.1161/01.cir.0000032901.55215.cc

Pashneh-Tala S, MacNeil S, Claeyssens F (2016) The tissue-engineered vascular graft—past, present, and future. Tissue Eng 22:68–100. https://doi.org/10.1089/ten.teb.2015.0100

Russell MW, Huse DM, Drowns S et al (1998) Direct medical costs of coronary artery disease in the United States. Am J Cardiol 81:1110–1115. https://doi.org/10.1016/S0002-9149(98)00136-2

Schmidt SP, Bowlin G, Schmidt SP, Bowlin GL (1999) Endothelial cell seeding: a review. In: Zilla P, Greisler HP (eds) Tissue engineering of vascular prosthetic grafts. R.G. Lanes Company, Austin, pp 61–67

Shabalovskaya SA, Siegismund D, Heurich E, Rettenmayr M (2013) Evaluation of wettability and surface energy of native Nitinol surfaces in relation to hemocompatibility. Mater Sci Eng C 33:127–132. https://doi.org/10.1016/j.msec.2012.08.018

Tiwari A, Salacinski H, Seifalian AM et al (2002) New prostheses for use in bypass grafts with special emphasis on polyurethanes. Cardiovasc Surg 10:191–197. https://doi.org/10.1016/S0967-2109(02)00004-2

Tsai WB, Grunkemeier JM, McFarland CD, Horbett TA (2002) Platelet adhesion to polystyrene-based surfaces preadsorbed with plasmas selectively depleted in fibrinogen, fibronectin, vitronectin, or von Willebrand's factor. J Biomed Mater Res 60:348–359. https://doi.org/10.1002/jbm.10048

Tukiainen E, Kallio M, Lepäntalo M (2006) Advanced leg salvage of the critically ischemic leg with major tissue loss by vascular and plastic surgeon teamwork: long-term outcome. Ann Surg 244:949–957. https://doi.org/10.1097/01.sla.0000247985.45541.e8

Uzarski JS, Van De Walle AB, McFetridge PS (2014) In vitro method for real-time, direct observation of cell-vascular graft interactions under simulated blood flow. Tissue Eng Part C 20:116–128. https://doi.org/10.1089/ten.tec.2012.0771

Virani SS, Alonso A, Aparicio HJ, Benjamin EJ, Bittencourt MSCC (2021) Heart disease and stroke statistics-2021 update a report from the American Heart Association. Circulation 135:e146–e603

Walgenbach KJ, Bannasch H, Kalthoff S, Rubin JP (2012) Randomized, prospective study of TissuGlu® surgical adhesive in the management of wound drainage following abdominoplasty. Aesthetic Plast Surg 36:491–496. https://doi.org/10.1007/S00266-011-9844-3

Wang X, Lin P, Yao Q, Chen C (2007) Development of small-diameter vascular grafts. World J Surg. https://doi.org/10.1007/s00268-006-0731-z

Wu XH, Liew YK, Mai CW, Then YY (2021) Potential of superhydrophobic surface for blood-contacting medical devices. Int J Mol Sci 22:3341

Zhang H, Dunphy DR, Jiang X et al (2012) Processing pathway dependence of amorphous silica nanoparticle toxicity: colloidal vs pyrolytic. J Am Chem Soc 134:15790–15804. https://doi.org/10.1021/ja304907c

Zhao Y, Sun X, Zhang G et al (2011) Interaction of mesoporous silica nanoparticles with human red blood cell membranes: size and surface effects. ACS Nano 5:1366–1375. https://doi.org/10.1021/nn103077k

Zhuang Y, Zhang C, Cheng M et al (2021) Challenges and strategies for in situ endothelialization and long-term lumen patency of vascular grafts. Bioact Mater 6:1791–1809